Heating Augmentation in Erosive Hypersonic Environments

Lyle E. Dunbar,* Joseph F. Courtney,† and Lowell D. McMillen†
Science Applications, Inc., El Segundo, Calif.

Heat transfer measurements in hypersonic particle erosion environments have indicated heating levels far in excess of clear air values for blunt models. Analyses have shown the primary heating augmentation mechanism to be convective heating due to particle distortions of the aerodynamic flowfield. A secondary mechanism is the particle kinetic energy conversion to model thermal energy. An empirical correlation has been developed for the stagnation region heat transfer to materials in erosive hypersonic environments. The convective heating Stanton number has been found to be independent of model geometry. It has been correlated as a function of particle to freestream air mass flux ratio.

Nomenclature

c = specific heat
$\dot{e}$ = particle kinetic energy flux
G = mass loss ratio
h = heat transfer coefficient
H = enthalpy
M = Mach number
P = pressure
q = heat transfer rate
Re = Reynolds number
St = Stanton number
t = time
T = temperature
V = velocity
ρ = density
χ = correlation parameter for convective Stanton number
δ = model skin thickness
ϕ = azimuthal angle from stagnation streamline

Subscripts

bf = backface
$cond$ = conduction
ff = frontface
g = gas
m = model material
o = stagnation conditions
p = dust particle
rad = radiation
w = wall conditions
∞ = freestream condition

I. Introduction

In early 1972, a series of tests were performed in the Arnold Engineering Development Center Dust Erosion Tunnel (AEDC DET) to evaluate the performance of titanium models in an erosive hypersonic environment. Measurements showed increased stagnation region heat transfer rates in these environments far in excess of "clear air" values. The increased heat transfer—termed "heating augmentation"—was in some cases sufficient to lead to titanium model ignition and burning. An extensive experimental and analytical study of heating augmentation mechanisms in erosive environments was initiated.

The initial phase of heating augmentation tests was performed in the AEDC DET[1] and the Boeing Hypersonic Wind Tunnel (BHWT).[2] These facilities were designed for particle erosion testing in hypersonic aerodynamic flow environments. The primary model materials were titanium, stainless steel, molybdenum, silver, and Inconel. Models were of thin-skin hemispheres and disks. Test data consisted of shadowgraph films and backface thermocouple temperature-time histories from which heat transfer data were derived.

Extensive data analyses as well as analytical studies[3] identified two primary heating augmentation mechanisms for metallic materials: 1) increased convective heating due to particle-induced distortions to the blunt model aerodynamic flowfield; and 2) conversion of incident particle kinetic energy to thermal energy in the model material. A third mechanism, peculiar to titanium, was identified as increased solid-state oxidation reactions at high surface temperatures ($\sim$2500°R) which lead to titanium ignition and burning. Analyses of this early data are contained in Refs. 4-6.

The kinetic energy transfer mechanism was expected although the fraction transferred to model thermal energy was unknown. However, the convective heating mechanism was an unexpected phenomena. This mechanism is believed to be related to distortions of the model bow shock layer observed in shadowgraph films. A sequence of frames from a shadowgraph film of a BHWT dust particle heating augmentation[6] test is shown in Fig. 1. The model is a disk in a Mach 6.1 flow with 100 μ diam silicon carbide (SiC) particles impacting at 2920 fps. The time between these successive frames is 1 msec and the shutter is open for 0.2 msec. The normal bow shock is observed in frames one and three with a severe conical distortion of the bow shock observed in frame number two. A similar phenomena is also observed for hemispherical models. Figure 2 illustrates the bow shock structure for a 3.0 in. diameter model in the BHWT for both a clear air environment and a dust particle environment. A major bow shock distortion is illustrated when the particle flow is initiated. These bow shock distortions occur somewhat randomly over the model stagnation region and are observed to occur about 10-20% of the test time. They are believed to be related to rebounding particles and surface debris interaction with the shock layer.

Presented as Paper 74-607 at the AIAA 8th Aerodynamic Testing Conference, Bethesda, Maryland, July 8-10, 1974; submitted August 5, 1974; revision received November 11, 1974. This work was supported by Air Force Contract F04701-73-C-0095 under the direction of Major L. J. Hudack, SAMSO Project Officer, and Defense Nuclear Agency Contract DNA001-73-C-0111 under the direction of M. J. Rubenstein. The contributions of H. R. Wilkinson of TRW Systems Group to the formulation of the empirical correlations is acknowledged.

Index categories: LV/M Aerodynamic Heating; Hypervelocity Impact; Material Ablation.

*Assistant Manager, Los Angeles Division.
†Staff Scientist. Member AIAA.

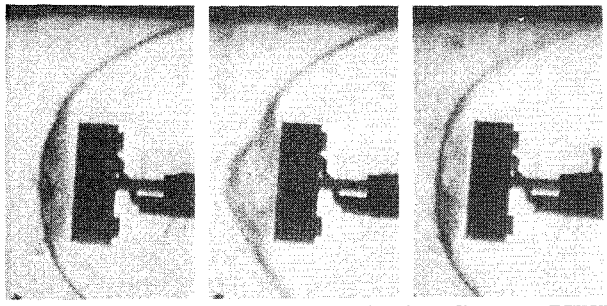

Fig. 1 Particle-induced flowfield distortion for a disk in the BHWT.

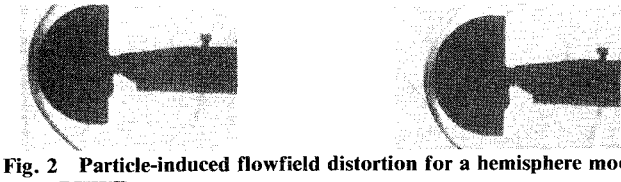

Fig. 2 Particle-induced flowfield distortion for a hemisphere model in the BHWT.

The kinetic energy transfer and convective heating augmentation mechanisms were inherently coupled in the experimental AEDC DET and BHWT data. An independent series of tests was performed using the SAI Hypervelocity Impact Facility to isolate the kinetic energy transfer mechanism. The results of these tests showed 70% kinetic energy transfer to target thermal energy for normal impacts of 100-200 μ diam particles on titanium targets at 3000-8000 fps impact velocities.[3] These tests adequately simulated the impact conditions for the AEDC DET and BHWT coupled tests. The 70% kinetic energy transfer fraction was verified independently considering equilibrium model temperatures reached in BHWT dust erosion tests.[6] Utilization of this result in conjunction with the AEDC DET and BHWT data provides a means for investigating the convective heating contribution.

A "coupled effects" follow-on test program was performed in the AEDC DET for a wide range of materials and test conditions to specifically investigate the convective heating augmentation mechanism and the coupled effects of kinetic energy transfer and convective heating.[7,8] A description of the AEDC DET coupled effects test program is presented in Sec. II.

II. Coupled Effects Heating Augmentation Test Program

Coupled effects heat transfer data were obtained from the AEDC Dust Erosion Tunnel (AEDC DET). A complete description of the AEDC DET facility is presented in Ref. 9.

AEDC DET Test Conditions

The AEDC DET is a modified arc heater designed specifically for the purpose of producing a hypervelocity particle erosion environment. The DET utilizes a 5 Mw high pressure Linde tubular electrode arc heater to provide operating gas (air) at a maximum nominal enthalpy of 1800 Btu/lb. A low-angle triconic nozzle configuration was designed for efficient dust particle acceleration. Two nozzle configurations—a standard nozzle length (207 in.) and a modified nozzle length (127.5 in.)—were used to obtain a variation in test section conditions. Test models were mounted on a rotating sting which allows for up to nine different models during a test run.

Particles were injected into the aerodynamic flow through a small tube installed in a water-cooled injector strut located in the tunnel stagnation chamber. The primary particulate used in the AEDC DET was magnesium oxide (MgO) because of its excellent high-temperature properties. However, silicon carbide (SiC) and glass particles were also used for some of the less severe thermal environment runs. A nominal 100 μ diam particulate is used with a few tests performed using 200 μ and 650 μ glass particulates to evaluate size effects. Particle velocities vary with test conditions. The particle velocities were initially obtained analytically using drag calculations. Double-pulsed optical holography was later used to experimentally determine particle velocities. Figure 3 shows the comparison of analytical and experimental particle velocities for the standard nozzle configuration.

Test models consisted of 1.0, 2.0, and 3.0-in. diam thin-skin hemispheres and 2.0-in. diam thin-skin disks. Models were designed with uniform skin thicknesses of 0.04 to 0.09 in. The hemisphere models were titanium (6A1-4V), Inconel, stainless steel and platinum. The disk models were titanium and graphite. Basic data consisted of temperature-time histories from backface thermocouples (platinum/platinum rhodium or chromel alumel type) and shadowgraph films of the model flowfield.

Experimental Data

Experimental data were obtained from the AEDC DET tests in the form of backface thermocouple temperature-time response for various model types, sizes, and test conditions. Typical data are shown in Fig. 4 for the stagnation temperature (backface) for a 3.0-in. diam titanium hemisphere model. The open symbols correspond to a "clear air" run from which the baseline heat transfer rates were established and the solid symbols correspond to the stagnation point measurement for a particle erosion run.

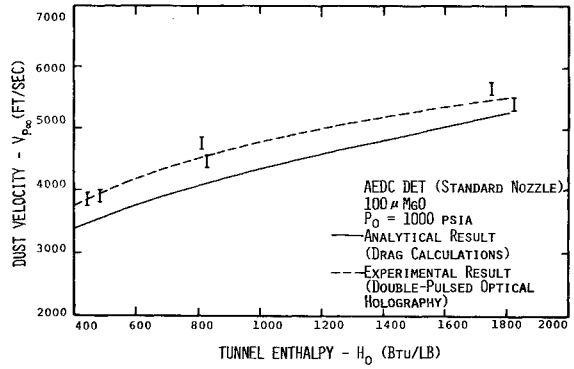

Fig. 3 AEDC DET dust particle velocity.

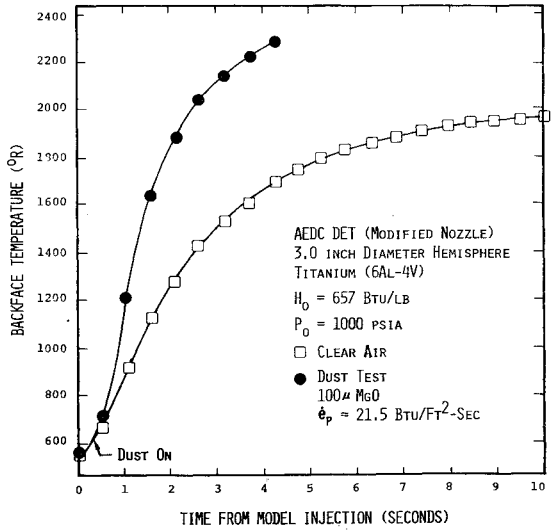

Fig. 4 Backface temperature response.

The backface temperature data are reduced to heat transfer rates using the thin-skin calorimeter equation. Corrections are made for front and backface radiation and lateral conduction. The net surface heat transfer rate is given by

$$\dot{q}_w = \rho_m \mathcal{L}_m \delta \, dT/dt + \dot{q}_{\text{rad},ff} + \dot{q}_{\text{rad},bf} + \dot{q}_{\text{cond}}$$

The stagnation point heat transfer rate corresponding to the data in Fig. 4 is shown in Fig. 5 as a function of wall temperature. The results show heat transfer rate increases by factors of 2-4 at the stagnation point of the 3.0-in. diam titanium hemisphere. This heat transfer augmentation is the combined result of kinetic energy transfer and convective heating augmentation due to particle/debris distortion of the model flowfield. The incident particle kinetic energy for the test in Fig. 5 was 21.5 Btu/ft^2-sec. Assuming straight line fits to the data and using 70% kinetic energy transfer, it is shown that the stagnation point convective heat transfer coefficient increases by a factor of 2.4 from 0.024-0.058 Btu/ft^2-sec-°R. The 70% kinetic energy transfer assumption is verified by the indicated heating rate at the tunnel total temperature (15 Btu/ft^2-sec) where the convective contribution is zero.

The effect of model size is shown in Fig. 6. The stagnation point heating rate is shown as a function of wall temperature for 1.0 and 3.0-in. diam titanium hemispheres. The laminar stagnation point heat transfer rate dependency on model nose radius (square-root dependence), clearly observed for the clear air tests and for the pre-dust period of the tests, disappears when the dust is turned on. Thus, blunt and sharp models have the same stagnation point heating level in particle environments. This phenomena is believed related to the distortions of the model flowfield which tend to eliminate the influence of the body geometry. The increase in heat transfer at temperatures of 2000-2500°R is due to solid-state chemical reactions in the titanium which ultimately lead to model ignition.

The heating augmentation phenomena is peculiar to blunt models but is not limited to the stagnation point. Figure 7 shows the heat transfer distributions in clear air and dust environments for the 1.0 and 3.0-in. diam titanium hemispheres. This data also shows the lack of influence of model geometry for off-stagnation locations.

The level of measured heating augmentation on other metallic materials, such as Inconel, stainless steel, and platinum, was found to be the same as titanium. However, tests using thin-skin graphite (ATJ-S grade) disks showed higher heating levels compared to titanium disks. Figure 8 shows the comparison of clear air and dust environment stagnation point heat transfer rates for the titanium and graphite disks. This was initially postulated to be a roughness effect since roughness heights can be greater for graphite compared to titanium. Tests proved this to be incorrect as shown in Fig. 9. The open symbols represent smooth wall graphite disks in a clear air environment. The solid symbols (triangles) were dust-roughened graphite models retested in a clear air environment. As the heat transfer levels indicate, roughness accounts for only a small fractrion of the measured heating rate for the graphite disk in the dust environment (solid square symbols). The increased graphite heat transfer rates compared to titanium are postulated to be the result of larger amounts of graphite debris distorting the model flowfield.

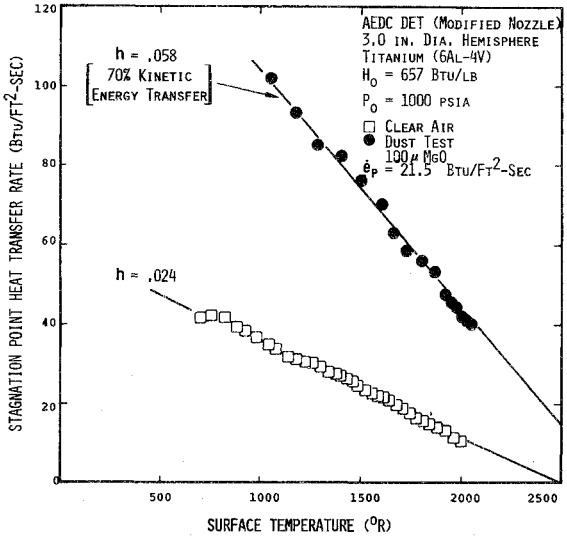

Fig. 5 Stagnation point heat transfer rates.

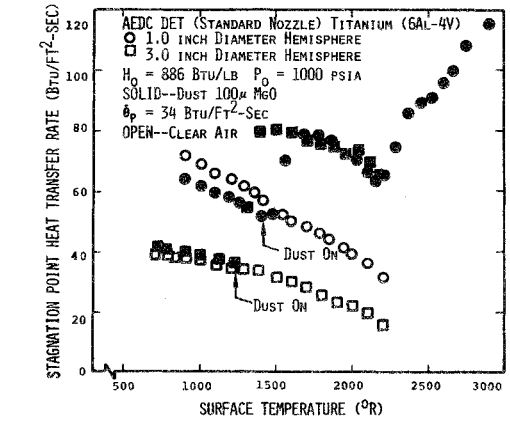

Fig. 6 Effect of model size on heating augmentation.

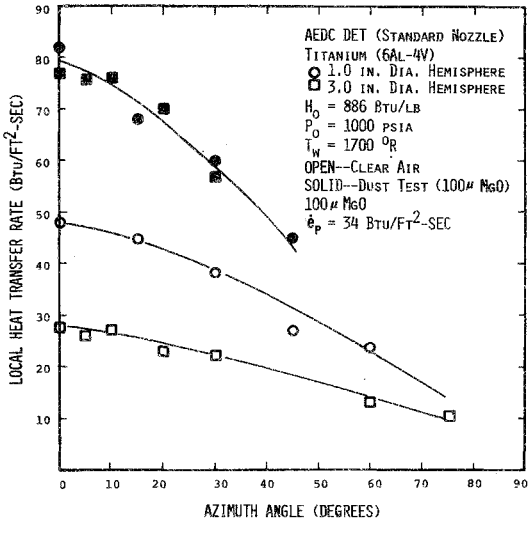

Fig. 7 Heat transfer distribution in clear air and dust environments.

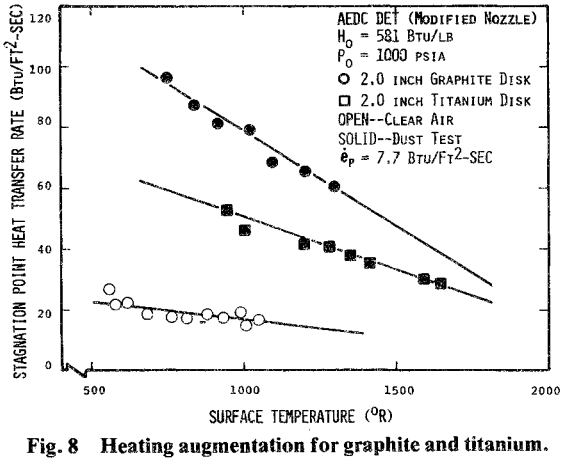

Fig. 8 Heating augmentation for graphite and titanium.

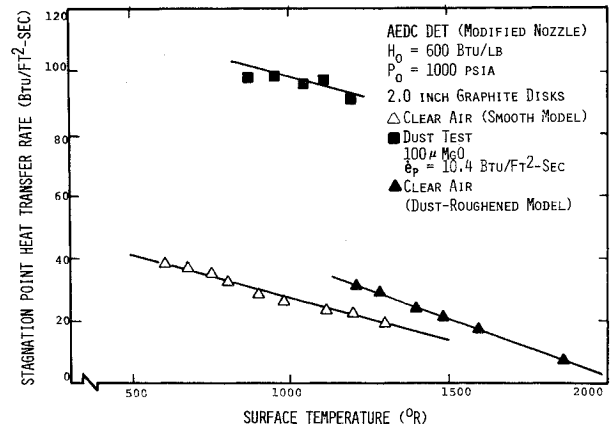

Fig. 9 Erosion-roughness contribution for graphite disks in a dust environment.

This phenomena had a predominant influence on subsequent data analysis and correlation of the convective heating augmentation data shown in Sec. III.

III. Convective Heating Augmentation Empirical Correlation

In Sec. II, the data presented from the AEDC DET contained the coupled effects of kinetic energy transfer and convective heating augmentation. The development of heat transfer models which could be extrapolated to flight conditions required the isolation and analysis of the individual mechanisms. The kinetic energy transfer mechanism was isolated in independent tests using the SAI Hypervelocity Impact Facility.[8] The 70% kinetic energy transfer function was derived from these tests and verified from BHWT equilibrium model temperatures in dust environments.[10] The coupled effects heating augmentation data base from the AEDC DET was then analyzed to isolate the convective heating mechanism. The approach adopted was to concentrate on the stagnation point data, extract the 70% kinetic energy transfer fraction, and correlate the remaining convective heating in the form of Stanton number (St) with test conditions and model characteristics. The Stanton number correlation for stagnation point heat transfer in particle erosion environments is derived from the expression

$$St=[\dot{q}_w-0.7(\dot{e}_p)]/\rho_{g\infty}V_{g\infty}(H_o-H_w)$$

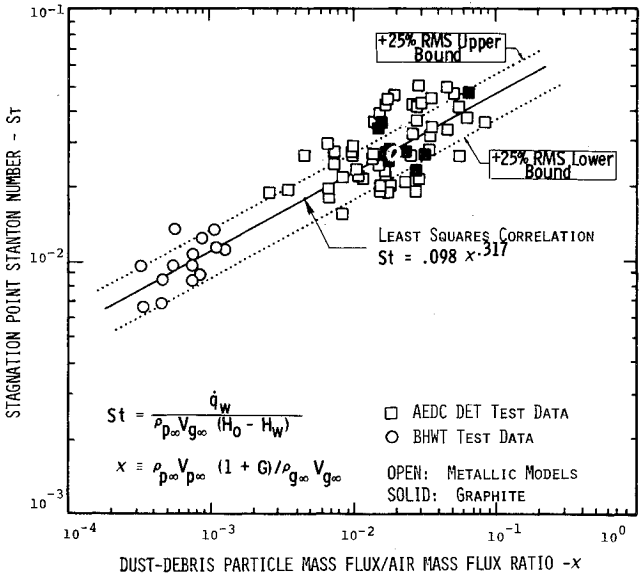

Fig. 10 Convective heating correlation.

The form of the correlation parameter was based on the following data trends for measured stagnation point heat transfer rates: 1) nose radius independence; 2) direct dependence on rebounding debris mass flux; and 3) inverse dependence on unit Reynolds number. The correlation paramter χ for the stagnation point Stanton number is defined as

$$\chi=\rho_{p\infty}V_{p\infty}(1+G)/\rho_{g\infty}V_{g\infty}$$

where G is the target material mass loss ratio (ratio of mass of target material eroded to impinging particle mass). Thus, this correlation parameter is the ratio of rebounding debris mass flux to air mass flux.

The final correlation for the stagnation point Stanton number is shown in Fig. 10. The least-squares correlation is $St=0.098\ \chi^{0.317}$. The ±25% rms error bounds are also shown. This correlation includes previous data obtained from the BHWT and the AEDC DET as well as the coupled effects test data from the AEDC DET. The correlation was obtained for the following ranges of parameters of interest:

$$6.1<M_\infty<9.5$$

$$0.135(10^6)<Re_\infty<18.8(10^6)\ \text{ft}^{-1}$$

$$2500<V_{p\infty}<5600\ \text{fps}$$

$$2.0<\dot{e}_p<58\ \text{Btu/ft}^2\text{-sec}$$

$$0.2<P_o<2\ \text{atm}$$

$$120<H_o<1800\ \text{Btu/lb}$$

IV. Conclusions and Recommendations

Measurements of heat transfer rates in hypersonic erosive environments indicate heating levels far in excess of clear air values. The primary heating augmentation mechanisms are: 1) convective heating due to particle distortions of the blunt model flowfield; and 2) kinetic energy transfer to target thermal energy. Detailed analyses and correlation of the convective heating augmentation test data indicate the following:

1) The convective heating Stanton number for the stagnation point of blunt models can be correlated with the ratio of dust/debris mass flux to air mass flux.

2) The convective heating augmentation contribution is independent of model nose radius.

3) Similar heating levels are measured for metallic materials but substantially higher levels are indicated for graphite in particle erosion environments.

4) Heat transfer distributions in particle environments have a cosine-squared azimuth angle dependence resulting in significant heat transfer increases at off-stagnation locations compared to clear air environments.

5) Erosion-induced surface roughness can be important for certain materials and particle sizes but was not a significant contributor to the measured stagnation point heating augmentation for small dust particle (100 μ) AEDC DET tests.

A considerable amount of progress has been made to date in modeling the heating augmentation of selected materials in erosive hypersonic environments. However, a number of important problems still remain to be addressed. The extrapolation of the empirical heating augmentation models to certain flight environments is limited by the current state of knowledge on the mechanism causing the increased convective heating. The limits of the empirical convective heating correlation for small and large values of the particle mass flux have not been defined. The coupling of the particle-induced convective heating model to rough wall heat transfer models has not been investigated. Finally, the effect of flowfield distortions on boundary-layer oxygen mass flux rates and thus material ablation rates has not been evaluated. Consideration must be given to these effects to develop a comprehensive

model for flight performance predictions of selected materials in particle erosion environments.

References

[1]Patton, J.B., et al., "SAMSO Material Evaluation, Block I," Letter Rept., Project PE0265, Sept. 1972, Arnold Engineering Development Center, Tullahoma, Tenn.

[2]Fleener, W., "Dust Augmented Convective Heating Test Data," personal communication, The Boeing Co., Seattle, Wash, Sept. 1972.

[3]Dunbar, L. E. and Courtney, J. F., "Minutemen Hot Structures Heating Augmentation Study, Vol. 1—Mechanisms and Analyses," SAMSO TR 73-272, Aug. 1973, Arnold Engineering Development Center, Tullahoma, Tenn.

[4]Dunbar, L. E., et al., "Minuteman Heating Augmentation Modeling Analyses," SAI-72-532-LA, Oct. 1972, Science Applications Inc., El Segundo, Calif.

[5]Burghart, G. H., "Evaluation of the AEDC Dust Erosion Tunnel Heat Augmentation Data," SAI-72-527-LA, Sept. 1972, Science Applications Inc., El Segundo, Calif.

[6]Fleener, W. A. and Watson, R. H., "Aerodynamic Heating in Dust-Laden Hypersonic Flows—Data Analysis Report," Boeing Doc. D2-26285-1, Jan. 1973, The Boeing Co., Seattle, Wash.

[7]Dunbar, L. E. and Courtney, J. F., "Minuteman Hot Structures Heating Augmentation Study, Vol. II—Coupled Effects Modeling," SAMSO TR-73-272, Aug. 1973, Space and Missiles Systems Organization, U.S. Air Force.

[8]Courtney, J. F., McMillen, L. D., Wenger, R. S., and Zuieback, J. M., "Heating Augmentation Phenomenology Studies," SAI-74-522-LA, April 1974, Science Applications Inc., El Segundo, Calif.

[9]Lewis, H. F., et al., "Description and Calibration Results of the AEDC Dust Erosion Tunnel, AEDC-TR-73-74, May 1973, Arnold Engineering Development Center, Tullahoma, Tenn.

[10]Fleener, W. A. and Watson, R. H., "Convective Heating in Dust-Laden Hypersonic Flows," AIAA Paper 73-761, Palm Springs, Calif., July, 1973.